Intersubband Auger recombination in a superlattice

Perng-fei Yuh and K. L. Wang
Device Research Laboratory, Department of Electrical Engineering, University of California, Los Angeles, California 90024-1600
(Received 19 August 1987)

It is known that the recombination mechanism in narrow-band-gap semiconductor lasers is dominated by the Auger process. An attempt to use the intersubband transitions in the superlattice for lasers is thus restricted by the Auger recombination process. The intersubband Auger recombination process is different from the conduction to valence-band Auger process since the subbands have different band structures, resulting in a different overlap integral and probability weighting function. The probability weighting function is comparable to that of the valence to conduction-band Auger process for narrow-band-gap (≤ 0.3 eV) bulk material. The overlap integral can be reduced by adjusting the miniband bandwidth. However, there is a tradeoff in controlling the bandwidth for a lower Auger rate (requiring narrower bandwidth) and for a larger carrier injection (requiring wider bandwidth). A closed form of the intersubband Auger rate is derived. It gives a much weaker band-gap and temperature dependence. Due to the adjustable overlap integral, the intersubband Auger rate can be made much lower than that of the conventional conduction to valence-band transition of the same band gap.

I. INTRODUCTION

The physics of intersubband optical transitions in quantum well structures and the device applications have been extensively studied by many authors.[1-10] The term "intersubband transitions" is used to refer to the subband-to-subband transitions occurring within only the condition subbands or within only the valence subbands. The intersubband optical transitions have many unique features as compared to the usual valence- to conduction-band transitions. First, the absorption or gain coefficient is sharp, analogous to an atomic two-level system. Second, the subband-to-subband energy gaps as well as the bandwidths can be tuned. The intersubband in superlattices can be treated as a man-made narrow-band-gap material with almost arbitrarily controllable parameters. Indirect-band-gap material such as Si and Ge can be used for lasing and it occurs as "direct" transition regardless of the nature of the host bulk material.

In order to access the merits of the intersubband transition for lasers, two problems remain to be solved. One is the pumping for population inversion; the other is the reduction of nonradiative recombination rates. The formal will be discussed briefly later. As for the nonradiative recombination process, we first consider the transition energies of intersubband transitions, which are typically on the order or less than a few tenths of eV, corresponding to the transition frequency in the infrared range. In narrow-band-gap semiconductor laser material, however, the nonradiative decay of the injected carriers at the lasing condition is dominated by the band-to-band Auger recombination.[11] It is thus important to study the Auger process in the intersubband transition in superlattices. This paper proceeds to analyze the dominant nonradiative Auger recombination process.

The fundamental theory of the Auger recombination was first treated by Beattie and Landsberg.[12] Since then several authors have calculated the band-to-band Auger rates involving the light hole[13] and the split-off band hole.[14] More complex calculations for phonon-assisted, trap Auger and second-Auger processes have taken into account nonparabolic bands, Fermi statistics, and screening effects in the case of bulk semiconductors.[15-18] In this paper the intersubband Auger recombination was treated. It, however, is different from the above calculations in that the intersubband case has different band structures and a different overlap integral and a probability weighting function. The probability weighting function is shown to be comparable to the conduction-to-valence Auger process for narrow-band-gap cases; while the overlap integral can be reduced by adjusting the miniband bandwidth. An analytic form has been obtained for the intersubband Auger process, and it shows that the recombination has a much less band-gap and temperature dependence. From this formulation we show that the intersubband transition has a significantly lower Auger rate than the conventional semiconductor lasers of the same bandgap due to the adjustable overlap integral, although the Auger remains to be the dominant recombination process.

II. MATRIX ELEMENT

For a two-level system, all the possible Auger interactions are depicted in Fig. 1. In Fig. 1, 1(a) and 1(b) are the recombination processes, while 1(c) and 1(d) are their corresponding inverse processes, the impact ionization. If we consider the upper (U) level as a conduction band (C) and the lower level (L) as heavy-hole valence band (H), then processes 1(a) and 1(c) involve three states in the conduction band and one in the heavy-hole valence band, and are conventionally called the *CHCC* process. Similarly, 1(b) and 1(d) are called the *CHHH* process.

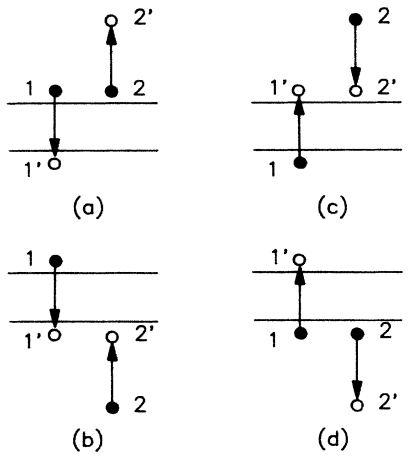

FIG. 1. All the possible transitions of two electron interaction in a two-level system. (a) and (c) are the *CHCC* process. (b) and (d) are the *CHHH* process. Each pair consists of one Auger process and one impact ionization. 1 and 2 are the initial states. 1′ and 2′ are the final states.

For the intersubband cases, they are referred as *ULUU* and *ULLL*, respectively.

Since the Auger recombination is a two-electron interaction via their Coulomb potential and it is a short-range interaction, the screened Coulomb potential is used.[19] The matrix element after summing over the singlet and triplet states of electrons 1 and 2 is of the following form:[12]

$$M_{if}=\int\int[\Phi_1^*(r_1)\Phi_2^*(r_2)\Delta_{21}-\Phi_2^*(r_1)\Phi_1^*(r_2)\Delta_{12}]\times[e^2\exp(-\lambda r_{12})/\epsilon r_{12}]\Phi_1'(r_1)\times\Phi_2'(r_2)d^3r_1\,d^3r_2\ , \tag{1}$$

where $\Phi_1(r_1),\Phi_2(r_2)$ denote the initial states of electrons 1 and 2, and $\Phi_1'(r_1),\Phi_2'(r_2)$ denote their final states. The quantities $\Delta_{21}=\Delta_{12}=1$ when electrons 1 and 2 have the same spins, preserved in the transition, $\Delta_{21}=1,\Delta_{12}=0$ when they have opposite spins preserved in the transition and $\Delta_{21}=0,\Delta_{12}=1$ when they have opposite spins but are both changed by the transition; $\Delta_{21}=\Delta_{12}=0$ otherwise. The quantity λ in the screened Coulomb potential is the reciprocity of the Debye length which is given by[15]

$$\lambda_B=\left[\frac{4\pi e^2n}{\epsilon kT}\right]^{1/2},\quad \lambda_F=\left[\frac{12m_ce^2n}{\epsilon\hbar^2}\right]^{1/2}\left[\frac{n}{9\pi}\right]^{1/6}, \tag{2}$$

for the Boltzmann and Fermi statistics, respectively. All the symbols have their usual definition. Using a two-band envelope function[20] in the growth direction $\hat{z}$, the superlattice wave function becomes

$$\Phi(k,q,r,z)=[F_s(q,z)u_s(k,q,r,z)+F_p(q,z)u_p(k,q,r,z)]e^{i\mathbf{k}\cdot\mathbf{r}}\ , \tag{3}$$

where $\mathbf{k}$ is the two-dimensional wave vector in the transverse direction, q is the wave vector along $\hat{z}$, and u_s and u_p are the periodic parts of the host Bloch functions for the conduction and light-hole bands, respectively. F_s and F_p are the envelope functions along $\hat{z}$. Using the Fourier expansion in the transverse direction as was done in Ref. 12, and neglecting the terms which have a product of two vanishing small (zero) terms in the overlap integrals, the matrix element for the *ULUU* process of the intersubband transition becomes

$$M_{if}=\frac{2\pi e^2}{\epsilon}\int\int\left[\frac{\Delta_{21}V(1,1')V(2,2')}{(g^2+\lambda^2)^{1/2}}-\frac{\Delta_{12}V(2,1')V(1,2')}{(h^2+\lambda^2)^{1/2}}\right]\times\delta(k_1+k_2-k_1'-k_2')dz_1dz_2\ , \tag{4}$$

where $g=|k_1-k_1'|$, $h=|k_1-k_2'|$, and the quantities $V(i,j)$ are defined by

$$\begin{aligned}V(1,1')&=F_U^*(q_1,z_1)F_L(q_1',z_1)\ ,\\ V(2,2')&=F_U^*(q_2,z_2)F_U(q_2',z_2)\ ,\\ V(2,1')&=F_U^*(q_2,z_1)F_L(q_1',z_1)\ ,\\ V(1,2')&=F_U^*(q_1,z_2)F_U(q_2',z_2)\ ,\end{aligned} \tag{5}$$

where F's are the F_s in Eq. (3) with U,L denoting the upper and lower levels, respectively. The terms involved with F_p are negligibly small, i.e., the one-band model is valid. For the conduction- to valence-band transition in quantum wells, $V(i,j)$ have the same definition as in Eq. (5) with F_U and F_L replaced by U_s and U_p and the integration is over r_1 and r_2. Thus the conduction- to valence-band transition in a quantum well has the same overlap integral as the bulk case[17] while the intersubband transition has an overlap integral determined only by the envelope functions, which can be easily tuned. In deriving Eq. (4), we have assumed that most of the contribution to the integral arises from small z_{12} (Ref. 17), i.e.,

$$\begin{aligned}&\int\frac{\exp[-\lambda(r_{12}^2+z_{12}^2)]^{1/2}}{(r_{12}^2+z_{12}^2)^{1/2}}\exp(-i\mathbf{r}_{12}\cdot\mathbf{g})r_{12}dr_{12}d\theta\\ &\approx\int\frac{\exp(-\lambda r_{12})}{r_{12}}\exp(-ir_{12}g\cos\theta)r_{12}dr_{12}d\theta\\ &=\frac{2\pi}{(g^2+\lambda^2)^{1/2}}\ .\end{aligned} \tag{6}$$

For the *ULLL* process, the matrix element is the same as Eq. (4) except that $V(i,j)$ are replaced by

$$\begin{aligned}V(1,1')&=F_U^*(q_1,z_1)F_L(q_1',z_1)\ ,\\ V(2,2')&=F_L^*(q_2,z_2)F_L(q_2',z_2)\ ,\\ V(2,1')&=F_L^*(q_2,z_1)F_L(q_1',z_1)\ ,\\ V(1,2')&=F_U^*(q_1,z_2)F_L(q_2',z_2)\ .\end{aligned} \tag{7}$$

In the discussion above, we have considered only the transitions involving two minibands, i.e., an ideal two-level system. If, however, either one of the four states involved in the process are in the third band, there will be a product of two negligible small terms in the overlap integral. The transitions involving three bands are thus treated as forbidden in the first-order approximation.

As discussed in Ref. 21, an upper bound for the matrix element of Eq. (4) may be written as

$$|M_{if}|^2 \leq 8\left[\frac{2\pi e^2}{\epsilon}\right]^2 \frac{\left|\int\int V(1,1')V(2,2')dz_1dz_2\right|^2}{g^2+\lambda^2}, \tag{8}$$

where g may be replaced by k_2' for the most probable transition so that the integration can be evaluated easily.

III. OVERLAP INTEGRAL

The overlap integral in Eq. (8) can be evaluated by constructing the superlattice envelope function $F(q,z)$ in terms of the isolated quantum well wave function $f_0(z)$ by a tight-binding scheme,[20]

$$F(q,z)=\frac{1}{\sqrt{N}}\sum_{j=-\infty}^{\infty} e^{iqjd}f_0(z-jd), \tag{9}$$

where d is the period of the superlattice and N is the number of periods in the superlattice. The conservation of momentum is required for nonzero results; thus we may write the overlap integral as

$$\begin{aligned}\int V(1,1')d\hat{z}_1 &= \int F_U^*(q_1,z_1)F_L(q_1',z_1)dz_1 \\ &= \int F_U^*(q_1,z_1)F_L(q_1',z_1)\delta(q_1-q_1')dz_1 \\ &= \sum_p 2\cos(pq_1d)\int f_{U0}(z_1)f_{L0} \\ &\quad \times(z_1+pd)dz_1 .\end{aligned}$$

Similarly, we have

$$\int V(2,2')dz_2=\int F_U^*(q_2,z_2)F_U(q_2',z_2)dz_2\approx 1 . \tag{10}$$

We notice that the miniband bandwidth is approximated to be[20]

$$B=4\int_{-\infty}^{\infty} f_0(z)V_c(z)f_0(z-d)dz , \tag{11}$$

where V_c is the conduction-band offset of the heterojunction making up the superlattice. For a square-well superlattice, the overlap integral can then be approximated by

$$\int\int V(1,1')V(2,2')dz_1dz_2\approx\frac{\sqrt{B_UB_L}}{2V_c}\cos(q_1d) , \tag{12}$$

where B_U,B_L is the miniband bandwidth for the upper and lower bands, respectively. For a parabola well as in the doped superlattice, the wave function may be approximated by the simple harmonic-oscillator model,[22]

$$F_j(z)=\pi^{-1/4}\alpha^{-1/2}e^{-z/2\alpha}(2^jj!)^{-1/2}H_j\left[\frac{z}{\alpha}\right], \tag{13}$$

where $\alpha^2=\hbar/m_c\omega_0$, $\omega_0=(e^2N_d/\epsilon m_c)^{1/2}$, and N_d is the doping. The two lowest-order Hermite polynomials are $H_0(x)=1, H_1(x)=2x$. Then the overlap integral becomes

$$\int\int V(1,1')V(2,2')dz_1dz_2=\frac{\sqrt{2}d}{\alpha}e^{-d^2/4\alpha^2}\cos(q_1d) . \tag{14}$$

IV. PROBABILITY WEIGHTING FUNCTION

Using Fermi's golden rule, the Auger rate is

$$\begin{aligned}R=\frac{2\pi}{\hbar}\left[\frac{1}{8\pi^3}\right]^4\int |M_{if}|^2P(1,1',2,2')\delta(E_i-E_f) \\ \times d^2k_1\,d^2k_2\,d^2k_1'\,d^2k_2'\,dq_1 \\ \times dq_2\,dq_1'dq_2' ,\end{aligned} \tag{15}$$

where P is the difference of the probabilities of the Auger process and the inverse process. In the following we will derive the most probable transition probability for different intersubband as well as the conventional band cases.

A. Case 1: *CHCC* for conventional band

Let us assume that all the energy levels are referenced to the valence-band maximum. For a conventional band in Fig. 2(a), the probability weighting function is

$$\begin{aligned}P&=(1\text{ occupied})(2\text{ occupied})(1'\text{ empty})(2'\text{ empty}) \\ &\quad -(1\text{ empty})(2\text{ empty})(1'\text{ occupied})(2'\text{ occupied}) \\ &=\frac{1-\exp-(E_{f_2}-E_{f_1})/kT}{(1+\exp(E_1-E_{f_2})/kT)[1+\exp(E_2-E_{f_2})/kT][1+\exp-(E_1'-E_{f_1})/kT]} ,\end{aligned} \tag{16}$$

where Fermi-Dirac distributions are assumed for quasiequilibrium, and E_{f_2},E_{f_1} are the quasi-Fermi-levels for the upper and lower levels, respectively. In the nondegenerate limit, Eq. (16) reduces to

$$P=e^{-E_2'/kT}e^{2E_{f_2}/kT}(1-e^{-(E_{f_2}-E_{f_1})/kT}) . \tag{17}$$

The maximum of P is obtained by minimizing E_2' with the constraint that both energy and momentum are con-

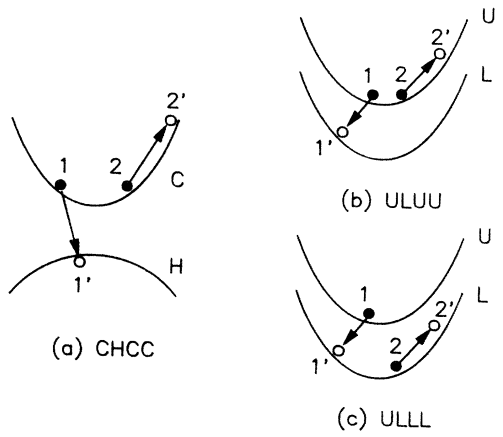

FIG. 2. (a) *CHCC* process in conventional band. (b) *ULUU* process in intersubband, corresponding to the *CHCC* process in the bulk case. (c) *ULLL* process in intersubband, corresponding to the *CHHH* process in the bulk case.

served. The result for the nondegenerate case is[12]

$$P_{\max}=\exp\left[-\frac{\mu}{\mu+1}E_G/kT\right]e^{-2(E_G-E_{f_2})/kT}\times(1-e^{-(E_{f_2}-E_{f_1})/kT}), \tag{18}$$

where $\mu=m_c/m_v$ is the ratio of effective masses of electrons and holes. The prefactor $\exp[-(\mu/\mu+1)E_G/kT]$ is the major cause of the band-gap and temperature dependence of the Auger rate. The rate of *CHCC* is usually larger than *CLCC*, where *L* stands for the light hole, simply because μ is smaller in *CHCC*. For the degenerate case, one may also assume that $P_{\max}$ occurs at the same condition as in the nondegenerate case such that

$$E_1'=-\frac{\mu}{(2\mu+1)(\mu+1)}E_G\ ,\qquad E_2=E_1=E_G+\frac{\mu^2}{(2\mu+1)(\mu+1)}E_G\ . \tag{19}$$

B. Case 2: *ULUU* for intersubband

For the band shown in Fig. 2(b), in the lasing condition we will assume states 1,2 in degenerate while states 1',2' in nondegenerate for simplicity. This case corresponds to the *CHCC* process in the conventional band. The probability function is

$$P=\frac{1-\exp-(E_{f_2}-E_{f_1})/kT}{[1+\exp(E_1-E_{f_2})/kT][1+\exp(E_2-E_{f_2})/kT]}\ , \tag{20}$$

whose maximum value $P_{\max}$ occurs at $E_2=E_1=E_G$, $E_2'=3/2E_G$, $E_1'=1/2E_G$. In the nondegenerate limit, we have

$$P_{\max}=e^{-2(E_G-E_{f_2}/kT)}(1-e^{-(E_{f_2}-E_{f_1})/kT})\ . \tag{21}$$

Compared to Eq. (18), the intersubband transition has a much larger probability than the conduction- to valence-band transition, especially for wide band-gap material at low temperature. However, for the narrow band-gap material in the lasing condition (usually in degenerate case), they are comparable. For example, for $E_G=0.1$, $\mu=0.15$, and $E_{f_2}-E_G=0.05$ eV, the ratio of $P_{\max}$ for interband and conventional band transitions are 1.3 at 300 K and 1 at 77 K.

C. Case 3: *ULLL* for intersubband

For the *ULLL* process shown in Fig. 2(c), which corresponds to the *CHHH* process in the bulk case, the probability is

$$P=\frac{\exp-(E_2-E_{f_1})/kT}{1+\exp(E_1-E_{f_2})/kT}[1-\exp-(E_{f_2}-E_{f_1})/kT]\ . \tag{22}$$

Here we assume that electrons in state 1 are degenerate while those in others are treated as nondegenerate. $P_{\max}$ occurs at $E_1=E_G$, $E_2=0$,

$$P_{\max}=\frac{e^{E_{f_1}/kT}}{1+e^{-(E_G-E_{f_2})/kT}}\ll 1\ . \tag{23}$$

If $E_{f_1}\ll 0$, then $P_{\max}$ for the *ULLL* process is much smaller than $P_{\max}$ for *ULUU*. This condition is usually valid in the intersubband transition. In the following calculation, we will consider only the *ULUU* process.

V. AUGER RATE AND DISCUSSION

The Auger rate is given by Eq. (15), where the matrix element $|M_{if}|^2$ is evaluated by Eq. (8) for the most probable transition, such that $g^2\approx k_2'^2\approx k_G^2/2$, where $E_G=\hbar^2k_G^2/2m_c$. Then the remaining part of the integration in Eq. (15) is

$$I=\int P(1,1',2,2')\delta(E_i-E_f)\delta(k_1+k_2-k_1'-k_2')\times\delta(q_1-q_1')\delta(q_2-q_2')d^2k_1\,d^2k_2\,d^2k_1'\,d^2k_2'\times dq_1\,dq_2\,dq_1'\,dq_2'\ , \tag{24}$$

where P is given by Eq. (20), and is only a function of E_1 and E_2, and all the delta functions come in when $|M_{if}|^2$ was evaluated. The difference of the initial and final energies taking the miniband energy into consideration is

$$E_i-E_f=E_1+E_2-E_1'-E_2'=\frac{\hbar^2}{2m_{c2}}(k_1^2+k_2^2+k_G^2+k_q^2-\mu k_1'^2-\mu_t k_2'^2)\ , \tag{25}$$

where $\mu=m_{c2}/m_{c1}$, $\mu_t=m_{c2}/m_{ct}$, and m_{c1} is the effective mass at the lower subband E_1, and m_{c2} and m_{ct} are those at E_2 and E_2', respectively; k_q is defined by

$$k_q = \left[\frac{m_{c2}}{\hbar^2}(B_U + B_L)\cos q_1 d \right]^{1/2} . \quad (26)$$

For the convenience of integration, two new variables $h = k_1' + k_2'$ and $j = k_1' - k_2'$ are introduced, and $m_{c1} = m_{c2} = m_{ct} = m_c$ are assumed. Then Eq. (25) becomes

$$\frac{\hbar^2}{2m_c}[k_1^2 + k_2^2 + k_G^2 + k_q^2 - \tfrac{1}{2}(|j|^2 + |k_1 + k_2|^2] . \quad (27)$$

The integration is then performed under the constraint

$$|j_0|^2 = 2(k_1^2 + k_2^2 + k_G^2 + k_q^2) - |k_1 + k_2|^2 \geq 0 , \quad (28)$$

which is always true if $E_G > B_U + B_L$. After integration with respect to k_1 and k_2, the final result for I becomes

$$I = \frac{32\pi^5 m_c N_{2D}^2}{\hbar^2}(1 - e^{-(E_{f_2} - E_{f_1})/kT}) , \quad (29)$$

where N_{2D} is the two-dimensional injected carrier concentration given by

$$N_{2D} = \frac{m_c kT}{\pi\hbar^2}\ln(1 + e^{(E_{f_2} - E_G)/kT}) . \quad (30)$$

Combining Eqs. (8), (12), and (29), the Auger rate (/sec·m^2) for the intersubband transition is then

$$R = \frac{m_c e^4}{\hbar^3 \epsilon^2}\frac{B_U B_L}{V_c^2}\frac{N_{2D}^2}{\lambda^2 + k_2'^2}(1 - e^{-(E_{f_2} - E_{f_1})/kT}) . \quad (31)$$

There again, B_U, B_L are the miniband bandwidth for the upper and lower bands, respectively, V_c is the conduction-band offset, λ is the reciprocal Debye length, and $k_2'^2$ is evaluated at the most probable transition such that $k_2'^2 \approx k_G^2/2$. The Auger recombination lifetime τ_{au}, defined by

$$R = \frac{N_{2D} - N_0}{\tau_{au}} \approx \frac{N_{2D}}{\tau_{au}}$$

is shown in Fig. 3 as a function of the subband band gap and N_0 is the equilibrium value. It is a linear function of the band gap, where the slope is inversely proportional to the injection carrier concentration. Compared to the conduction- to valence-band Auger recombination time, which has an exponential dependence of the band gap and the temperature, the intersubband Auger time has a smaller band-gap dependence and is constant in temperature. As a result the threshold current for intersubband laser transitions will have a much weaker temperature dependence. The spontaneous emission lifetime, given by the expression[23]

$$\frac{1}{\tau_{sp}} = \frac{2n^3\mu^2\omega^3 g_1}{\epsilon hc^3} \quad (32)$$

is also plotted in Fig. 3, where n is the index of refraction, g_1 is the degeneracy factor, and μ is the dipole moment given by

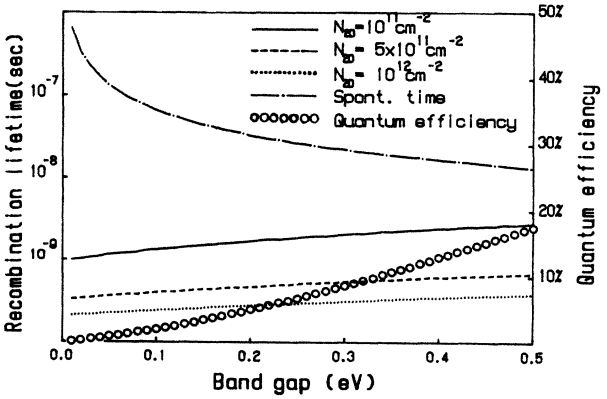

FIG. 3. The recombination lifetime vs energy band gap. Three lines are for intersubband Auger recombination time with different injection levels. They are increasing functions of the band gap. The spontaneous lifetime is a decreasing function of the band gap. The quantum efficiency is defined by Eq. (34) using the data of $N_{2D} = 10^{11}/cm^2$. All other parameters not specified in the text are assumed to be for GaAs.

$$\mu^2 = \frac{\hbar e^2}{2m_0\omega} f_{ij} , \quad (33)$$

where f_{ij} is the oscillator strength, assumed to be unity here. The spontaneous quantum efficiency η defined by

$$\eta = \frac{\tau_{au}}{\tau_{sp} + \tau_{au}} \quad (34)$$

is also plotted in Fig. 3 as a function of energy. The Auger recombination time as well as the quantum efficiency could be tailored by adjusting the miniband bandwidth. Here we assume that $B_U = 10$ meV, $B_L = 1$ meV, and $V_c = 0.24$ eV. However, the miniband bandwidth is limited by the accuracy of the growth parameters. Also, the choice of bandwidth is limited by the requirement for efficient injection. The effective mass in the growing direction of a superlattice is estimated to be $m_z = 2\hbar^2/Bd^2$.[24] As the bandwidth becomes small, the effective mass increases and the mobility drops. In the limiting case of quantum wells, the miniband bandwidth becomes zero and the Auger rate is zero. However, the current injection will then be impossible in this case since the mobility of the structure is zero.

As for the pumping in the intersubband lasing transition, one possible way is shown in Fig. 4.[25] The population inversion is achieved by current injected through the aligned superlattice minibands in the right-hand side. While in the left-hand side, the injected carriers are

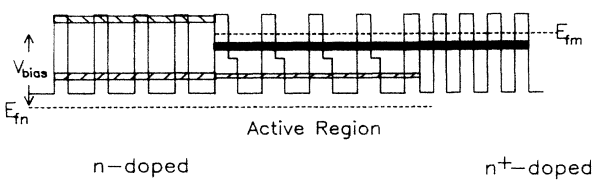

FIG. 4. Band-aligned superlattice laser using intersubband optical transition and miniband alignment.

blocked by the miniband discontinuity there. Such a band alignment scheme allows convenient current injection for the intersubband lasing.

VI. CONCLUSION

In conclusion, we have calculated the intersubband Auger recombination rate in superlattices. An analytic form is derived which shows much smaller band-gap and temperature dependence. With the promising of an adjustable Auger rate by choosing the superlattice parameters (composition, dopant, thickness, etc.), the intersubband Auger rate could be two orders of magnitude smaller than the conventional narrow band-gap material. High gain coefficient, smaller threshold current, less temperature dependence of the threshold current, and better tunability could be expected for the applications in long-wavelength lasers using intersubband transition in superlattices.

ACKNOWLEDGMENTS

The authors are indebted to Dr. J. Schulman for calculations relating to the superlattice miniband. This work is in part supported by the U.S. Office of Naval Research and the Semiconductor Research Corporation and the U.S. Army Research Office.

[1]B. Jogai and K. L. Wang (to be published).
[2]D. D. Coon and R. P. G. Karunasiri, Appl. Phys. Lett. **45**, 649 (1984).
[3]L. C. West and S. J. Eglash, Appl. Phys. Lett. **46**, 1156 (1985).
[4]D. D. Coon, R. P. G. Karunasiri, and L. Z. Liu, Appl. Phys. Lett. **47**, 289 (1985).
[5]D. D. Coon, R. P. G. Karunasiri, and L. Z. Liu, J. Appl. Phys. **60**, 2636 (1986).
[6]B. F. Levine, R. J. Malik, J. Walker, K. K. Choi, C. G. Bethea, D. A. Kleinman, and J. M. Vandenberg, Appl. Phys. Lett. **50**, 273 (1987).
[7]D. Ahn and S. L. Chuang, Phys. Rev. B **35**, 4149 (1987).
[8]Alex Harwit and J. S. Harris, Jr., Appl. Phys. Lett. **50**, 685 (1987).
[9]B. F. Levine, K. K. Choi, C. G. Bethea, J. Walker, and R. J. Malik, Appl. Phys. Lett. **50**, 1092 (1987).
[10]K. K. Choi, B. F. Levine, C. G. Bethea, J. Walker, and R. J. Malik, Appl. Phys. Lett. **50**, 1814 (1987).
[11]Yoshiji Horikoshi, in *Semiconductors and Semimetals,* edited by R. K. Willardson and A. C. Beer (Academic, London, 1985), Vol. 22, part C, pp. 93–151.
[12]A. R. Beattie and P. T. Landsberg, Proc. R. Soc. London Ser. A **249**, 16 (1959).
[13]A. R. Beattie and G. Smith, Phys. Status Solidi **19**, 577 (1967).
[14]M. Takeshima, J. Appl. Phys. **43**, 4114 (1972).
[15]Albert Haug, Solid-State Electron. **21**, 1281 (1978).
[16]N. K. Dutta and R. J. Nelson, J. Appl. Phys. **53**, 74 (1982).
[17]N. K. Dutta, J. Appl. Phys. **54**, 1236 (1983).
[18]R. I. Taylor, R. W. Kelsall, and R. A. Abram, Surf. Sci. **174**, 169 (1986).
[19]A. Haug, *Theoretical Solid State Physics* (Pergamon, Oxford, 1972), Vol. 2.
[20]G. Bastard, in *Molecular Beam Epitaxy and Heterostructures,* Vol. 87 of *NATO Advanced Study Institute, Series E: Applied Sciences,* edited by L. L. Chang and K. Ploog (Nijhoff, Dordrecht, 1985), pp. 381–423.
[21]Akira Sugimura, J. Appl. Phys. **51**, 4405 (1980).
[22]Gottfried H. Dohler and Peter Paul Ruden, Phys. Rev. B **30**, 5932 (1984).
[23]Amnon Yariv, *Quantum Electronics,* 2nd Ed. (Wiley, New York, 1975), Chap. 8.
[24]J. N. Schulman (private communication).
[25]Perng-fei Yuh and K. L. Wang, Appl. Phys. Lett. **51**, 1404 (1987).